Photometric Analyses and Spectral Identification of the Early-Spectral Type W UMa Contact Binary V444 Andromedae

Ronald G. Samec
Faculty Research Associate, Pisgah Astronomical Research Institute, One Pari Drive, Rosman, NC 28772; and Emmanuel College, 181 Springs St., PO Box 129, Franklin Springs,GA 30639; ronaldsamec@gmail.com

Russell Robb
University of Victoria, Department of Physics and Astronomy, P.O. Box 3055, Station CSC, Victoria, BC V8W 3P6, Canada; and Guest Observer, Dominion Astrophysical Observatory

Danny R. Faulkner
University of South Carolina, 476 Hubbard Drive, Lancaster, SC 29720

Walter Van Hamme
Florida International University, Department of Physics, 11200 SW 8th Street, Miami, FL 33199

Received October 31, 2014; revised December 9, 2014; accepted December 9, 2014

Abstract Presented here are the first precision UBVR$_c$I$_c$ light curves, synthetic light curve solutions, a period study, and spectrum for V444 Andromedae, an F0V contact W UMa binary. Observations were taken with the Lowell Observatory 0.81-m reflector during 28 through 30 September 2012. From our period study we determined a linear ephemeris showing that the period has been stable over the past 9.6 years (~7,500 orbits). The period during this interval is 0.46877942 d. After a q-search, the lowest residual mass ratio was found to be 0.48 with a Roche-lobe fill-out of nearly 51%. Despite its rather high temperature, 7,300 K, two magnetic spots were modeled on the primary component, a 10° radius equatorial dark spot with a T-factor of 0.88 and a 23° radius near-polar hot spot of T-factor 1.10. The component temperature difference was only ~80 K. These parameters point to a mature, early type, W UMa binary.

1. Introduction

W UMa variable stars are thought to reach contact starting from a detached stage of perhaps a 3- to 5- orbital days period (Yildiz 2014) and slowly reach contact and remain so over eons, steadily losing angular momentum via magnetic braking. Short period, P < 1/2 d, contact binaries are believed to be among the oldest stars in the galaxy (Yildiz 2014). They continue to coalesce with the secondary component losing mass to the primary in a contact Roche Lobe configuration, while steadily becoming more extreme in fill-out and in mass ratio, until the binary becomes a single star in a rapid, observationally-rare event. Ultimately, these binaries become an F to A–type fast rotating, single, blue straggler-like star (Jiang *et al.* 2014). Our studies have followed the stages through most of the cycle (Yakut and Eggleton 2005). This article gives a first analysis of such a binary, V444 Andromedae, apparently maturing in its contact stage.

2. Observational history

V444 Andromedae (MisV1097, GSC 02808-00139, USNO-A2.0 1275.00747331) is a MISAO Project Variable discovered by Seiichi Yoshida, Nobuo Ohkura, Okayama, Japan, and Ken-ichi Kadota (http://www.aerith.net/misao/data/misv.cgi?1097). Ondrej Pejcha (2005) classified it as a blue W UMa-type (EW/KE-type) eclipsing variable (Kazuhiro Nakajima's observations gave an unfiltered CCD light curve and estimated it to vary from 13.04 to 13.74 magnitudes, with a period of 0.4688 day (Nakajima *et al.* 2005). Times of minima observed by Ondrej Pejcha have been published (2005). Five times of minimum light are given in *Variable Star Bulletin No. 42* (Nagai 2004). V444 And is listed in the 78th *Name-List of Variable Stars* (Kazarovets *et al.* 2006) with position R.A. $01^h\ 15^m\ 28.7^s$ Dec. +41° 19' 59", and magnitude range of 13.0–13.7. It was classified as an EW binary. Finally, two times of minimum light were observed by Lewandowski *et al.* (2007).

3. The present observations

The V444 And system was observed as a part of our student/professional collaborative studies of interacting binaries taken from data at the NURO (National Undergraduate Research Observatory). The observations were taken by Dr. Ron Samec, Dr. Danny Falkner, Sharyl Monroe, and Heather A. Chamberlain. The reductions and analyses were done by Travis Shebs and Dr. Samec.

Our UBVRI light curves of V444 And were taken with the Lowell 31-inch reflector in Flagstaff, Arizona, with a CRYOTIGER cooled (< –100º C) NASACAM and a 2K × 2K chip (Plate Scale = 0.515 arcsec/pixel, http://www.nuro.nau.edu/specs.htm) and standard Johnson-Cousin BVR$_c$I$_c$ filters. They were observed on 28, 29, 30 September 2012. The light curves were subjected to synthetic light curve modeling. The observations included 48 in U filter, 128 in B, R$_c$, and I$_c$-filters,

Table 1. The variable (V), comparison (C), and check (K) stars in this study.

Star	*Name*	*R.A. (2000)* *h m s*	*Dec. (2000)* ° ′ ″	*V*	*Source**
V	V444 And GSC 2808 0139	01 15 28.72	+41 19 58.9	12.86	IRCS
C	GSC 2808 0101	01 15 52.759	+41 22 15.56	12.93	*Guide 9*
K	GSC 2808 0111	01 15 24.924	+41 18 43.23	12.13	*Guide 9*

**Guide 9 (Project Pluto 2012).*

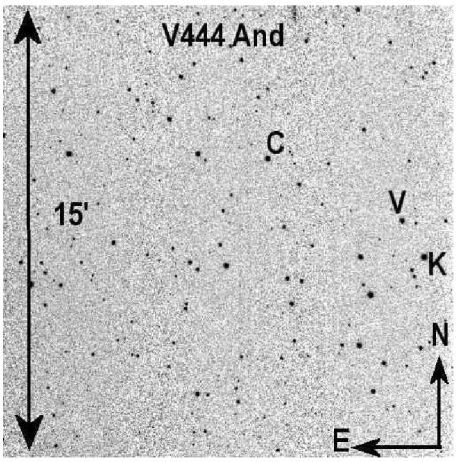

Figure 1. Finding chart for V444 And (V), comparison (C) and check (K).

and 127 in V, individual CCD observations. The standard errors of a single observation were 1.3 mmag in U, 7 mmag B and I, 4 mmag V, 4 mmag R_c. Typical exposure times were 300s in U, 75s in B, 50s in V, and 35s in R_c and I_c. Images were calibrated in a standard way using biases, 300-sec darks and UBVRI sky flats with AIP4WIN (Berry and Burnell 2011, CFITSIO package developed by NASA). The stars in this study (Table 1) are shown on the finding charts in Figure 1. The UBVRI observations in delta magnitudes, in the sense of V–C, are given online at http://smileycontrol.pari.edu/smileydata/Users/Samec/V444And .

4. Period determination

Three new times of minimum light were determined from our observations. These include:

JD Hel Min I = 2456199.0239 ± 0.0011,
2456199.9616 ± 0.0015,

and

JD Hel Min II = 2456198.7907 ± 0.0005.

From all available timings, an improved linear ephemeris was determined:

JD Hel Min I =
2456199.9618 ± 0.0003d + 0.46877942 ± 0.00000005 × E (1)

The O–C residuals calculated using Equation 1 are given along with all available timings and their O–C residuals in Table 2. The plot of residuals is given in Figure 2.

Table 2. O–C Residuals calculated from Equation 1.

	Epoch *JD 2400000+*	*Cycle*	*O–C*	*Reference*
1	52685.2892	–7497.5	0.0011	Nakajima *et al.* 2005
2	52911.0059	–7016.0	0.0005	Nakajima *et al.* 2005
3	52912.1761	–7013.5	–0.0013	Nakajima *et al.* 2005
4	52914.0532	–7009.5	0.0007	Nakajima *et al.* 2005
5	52914.2861	–7009.0	–0.0008	Nakajima *et al.* 2005
6	53966.6965	–4764.0	–0.0002	Diethelm 2007
7	53966.9314	–4763.5	0.0003	Diethelm 2007
8	54097.2513	–4485.5	–0.0005	Diethelm 2007
9	56198.7907	–2.5	0.0008	Present observations
10	56199.0239	–2.0	–0.0004	Present observations
11	56199.9616	0.0	–0.0002	Present observations

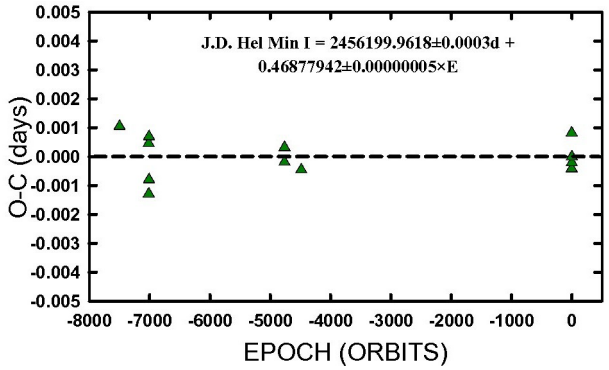

Figure 2. O–C linear residuals from period study and Equation 1.

5. Spectral type, temperature

Robb observed the spectrum of V444 And at Dominion Astrophysical Observatory (DAO) with the 1.8-m telescope at a dispersion of 60 Å/mm. The mid-time of exposure was 23 Jul 2013 10:20:03 UT and lasted 999 seconds which was at MJD 2456496.4181, corresponding to phase 0.48. The strengths of all lines indicate a F0V ± 1 (7,300 K) spectral type. The spectrum and the comparison spectrum of ρ Gem are given in Figure 3. The B–V for an F0V Star is ~0.3. From the AAVSO Photometric All-Sky Survey (APASS; Henden *et al.* 2013), B–V = 0.42. This gives a reddening of E(B–V) = 0.12.

6. Light curve characteristics

Phased light curves using Equation (1) to fold the light curves are given in Figures 4a, 4b, and 4c.

The ΔU to ΔI_c magnitude curve amplitudes are from 0.72 to 0.63 magnitude, respectively. Whereas, the O'Connell (MAXII-MAXI) effect is small as compared to the errors, it does

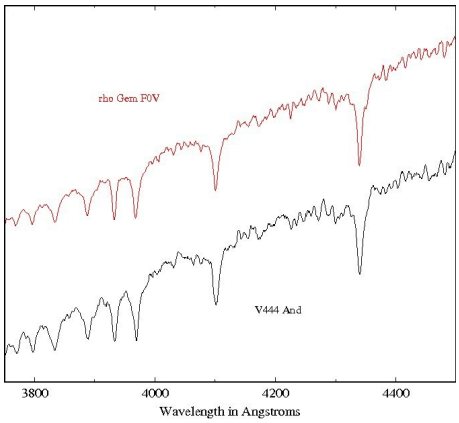

Figure 3. DAO spectra of V444 And and comparison star.

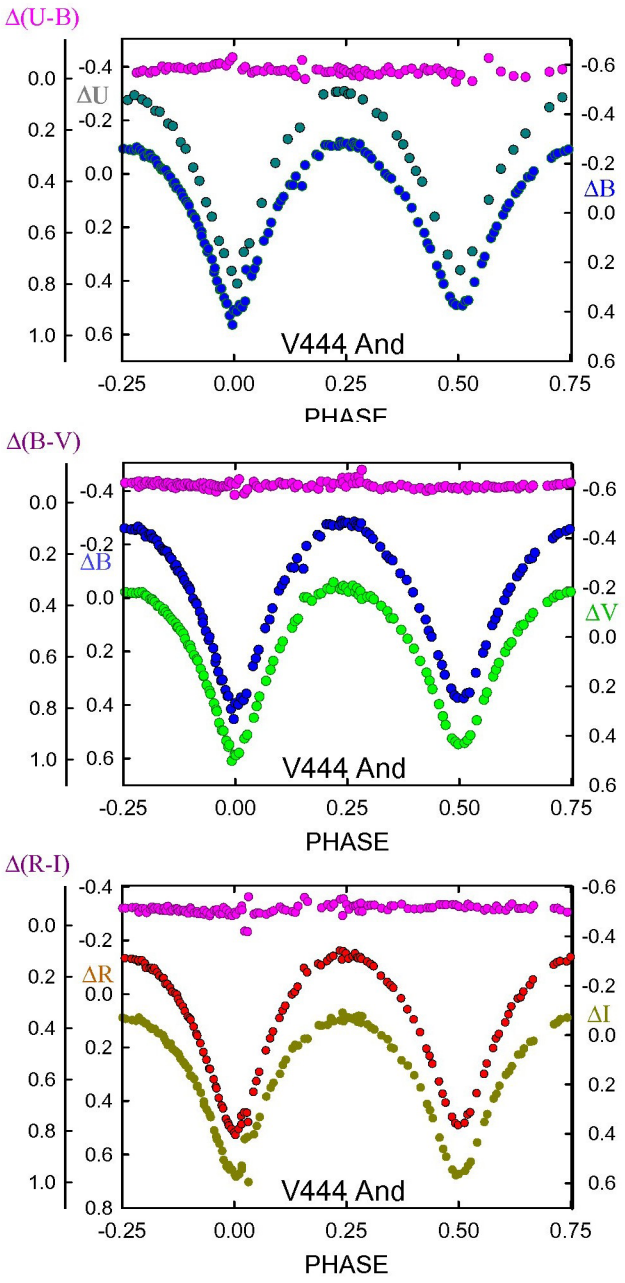

Figures 4a (top), 4b (middle), 4c (bottom). Phased ΔU, ΔB, ΔV, ΔR_c, and ΔI_c differential magnitude light curves and Δ(U–B), Δ(B–V), $\Delta(R_c–I_c)$ color curves.

Table 3. Light curve characteristics.

Filter	*Magnitude*	
	Max. I	*Max. II*
Phase	0.25	0.75
ΔU	–0.305±0.005	–0.285±0.013
ΔB	–0.278±0.007	–0.258±0.005
ΔV	–0.201±0.011	–0.179±0.003
ΔR	–0.149±0.013	–0.133±0.002
ΔI	–0.069±0.012	–0.064±0.004
Δ(U–B)	–0.027±0.012	–0.027±0.018
Δ(B–V)	–0.077±0.018	–0.078±0.007
Δ(R–I)	–0.072±0.025	–0.054±0.006
	Min. II	*Min. I*
Phase	0.5	0.0
ΔU	0.360 —	0.410 —
ΔB	0.371±0.006	0.400±0.028
ΔV	0.432±0.003	0.475±0.005
ΔR	0.485±0.004	0.515±0.011
ΔI	0.560±0.008	0.561±0.011
Δ(U–B)	–0.011±0.006	0.010±0.028
Δ(B–V)	–0.061±0.009	–0.075±0.033
Δ(R–I)	0.546±0.012	0.589±0.022

	Min. I–Max. I	*Min. II–Max. I*	*Min. I–Min. II*
ΔU	0.715±0.005	0.020±0.018	0.050±0.000
ΔB	0.678±0.035	0.021±0.012	0.029±0.034
ΔV	0.676±0.016	0.022±0.014	0.044±0.008
ΔR	0.664±0.024	0.017±0.015	0.030±0.015
ΔI	0.630±0.023	0.006±0.015	0.001±0.019
Δ(U–B)	0.037±0.040	–0.001±0.029	0.021±0.034
Δ(B–V)	0.002±0.051	–0.001±0.025	–0.014±0.042
Δ(R–I)	0.661±0.047	0.017±0.030	0.044±0.034

signal the presence of spots, averaging about 0.02 magnitude. The depths of eclipse are very nearly equal to within 0–5%, so the temperatures of the binary components are nearly identical. This is not unexpected for a high fill-out mature W UMa binary. The magnitude differences of the light curve characteristics at quadratures are given in Table 3.

7. Synthetic light curve modeling

Each filter's light curve was fitted, individually, with BINARY MAKER 3.0 (Bradstreet and Steelman 2002) using standard convective parameters and limb darkening coefficients from tabled values dictated by the spectral type. In these models we used both under-luminous and over-luminous spots to fit the asymmetries in the curves. Using our averaged values from BINARY MAKER and the primary component temperature from our spectrum (7,300 K), we proceeded to compute a UBVRI simultaneous five color light curve solution with the Wilson Devinney Program (Wilson and Devinney 1971; Wilson 1990, 1994; Van Hamme and Wilson 1998) includes Kurucz stellar atmospheres rather than black body. We used two-dimensional limb-darkening coefficients and a detailed reflection treatment in our modeling. Our fixed inputs included standard convective parameters: gravity darkening, g, = 0.32 and albedo value of 0.5. We used Mode 3 in our analysis (the contact configuration). Since the eclipses were not total, a q-search was prescribed. There is no third light in our solution. Only small negative and

negligible values resulted when it was included in the adjustable parameters, indicating that no third body of appreciable brightness contributes to the overall light of the system. So after a sufficient q-search, the lowest residual mass ratio was found to be 0.48. The residual vs. mass ratio plot is given in Figure 5. Adjustable parameters include those accompanied by errors (see Table 4), the inclination, i, the temperature of the secondary component, T2, the potential, Ω, the mass ratio, $q = M_2/M_1$, the normalized flux (at 4π) in each wavelength, L, the phasing ephemeris, JD_o, the period P, and the four spot parameters. Our complete solution is given in Table 4 and the curves are shown in Figures 6a and 6b, where the solution is overlying the normalized flux light curves. The Roche lobe surfaces arising from the calculation are displayed in Figures 7a, 7b, 7c, and 7d. We also calculated a nonspotted solution for comparison. Note that the sum of square residuals was 0.425 for the spotted solution and 0.601 for the unspotted one (41% larger). Finally, we calculated a radiative solution, with radiative parameters, gravity darkening, g, = 1.00 and albedo value of 1.0. The solution is given in Table 4. The main differences are the light-related phenomena and the fill-out which is substantial but smaller. The sum of square residuals was 0.425 for the convective solution and 0.579 for the radiative one (36% larger). So, the convective solution was best.

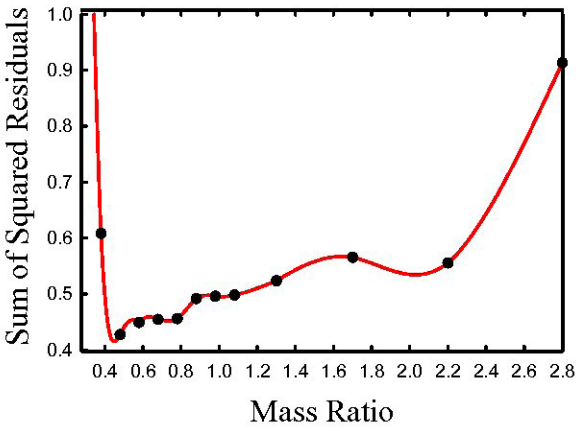

Figure 5. Mass ratio (q) search, fixed q-solutions vs. sum of square residuals to determine the best q-value.

8. Discussion

V444 And is an early-type contact W UMa system. It is of F0V spectral type. The period has been constant over the past 9.6 years. The orbital period during this interval is 0.46877942 d. The lowest residual mass ratio is found to be 0.48 and the fill-out is rather large, some 51%. Despite its temperature (7,300 K), two magnetic spots were modeled on the primary component, a small 10° radius equatorial dark spot, and a moderate-sized 23° radius hot polar spot. The inclination was above 80° so its eclipses are nearly total, with only 1–2% of the light contributed by the secondary component at phase 0.5. The component temperature difference is only ~80 K, so despite the disparate mass ratio, the components are in good thermal contact. Since the binary is magnetically active, we expect this system will eventually become a fast spinning early A-type star. The process of coalescence is caused by magnetic braking due to stellar winds leaving the system via stiff dipole magnetic field lines. We note that radial velocity curves are needed to confirm the mass ratio and to determine absolute mass values. In addition, this system should be patrolled for the next ten years or so to determine possible changes in the period behavior of the system.

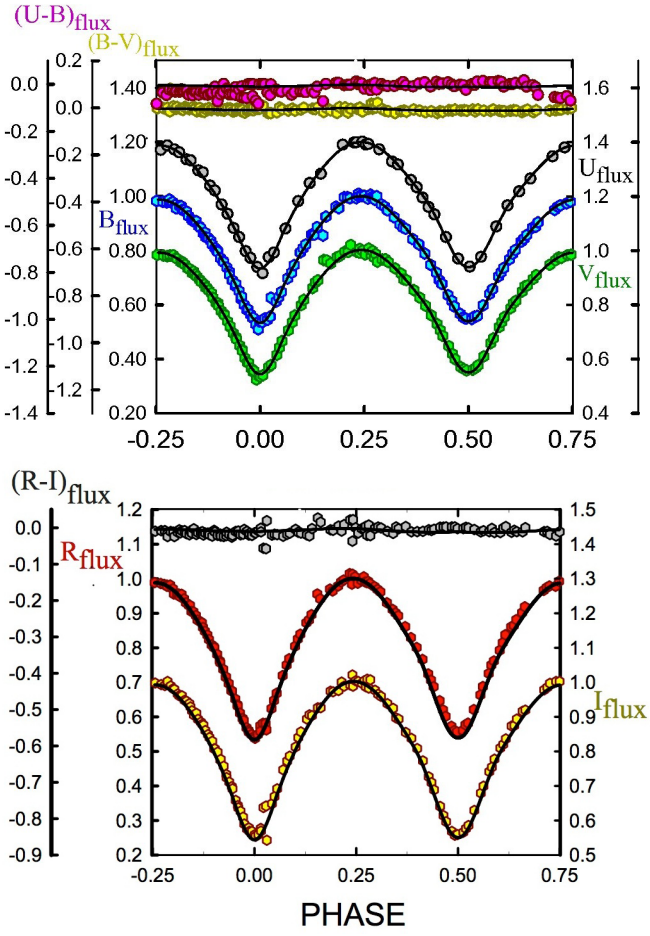

Figure 6a (top). U, B, V normalized flux curves overlain by our solution. Figure 6b (bottom). R_c, I_c normalized flux curves overlain by our solution.

9. Acknowledgements

We wish to thank NURO for their allocation of observing time and Bob Jones University for their support of our observing runs over the past eighteen years. We also wish to think Pisgah Astronomical Research Institute for appointing the primary author as a Faculty Research Associate. This research was made possible through the use of the AAVSO Photometric All-Sky Survey (APASS), funded by the Robert Martin Ayers Sciences Fund.

Table 4. V444 And, synthetic light curve solution.

Parameters	*Convective Solution*	*Radiative Solution*
λ_U, λ_B, λ_V, λ_R, λ_I (nm)	360, 440, 550, 640, 790	360, 440, 550, 640, 790
$x_{bol1,2}$, $y_{bol1,2}$	0.642, 0.642, 0.260, 0.260	0.642, 0.642, 0.260, 0.260
$x_{1I,2I}$, $y_{1I,2I}$	0.517, 0.517, 0.283, 0.283	0.517, 0.517, 0.283, 0.283
$x_{1R,2R}$, $y_{1R,2R}$	0.604, 0.604, 0.300, 0.300	0.604, 0.604, 0.300, 0.300
$x_{1V,2V}$, $y_{1V,2V}$	0.683, 0.683, 0.298, 0.298	0.683, 0.683, 0.298, 0.298
$x_{1B,2B}$, $y_{1B,2B}$	0.782, 0.782, 0.300, 0.300	0.782, 0.782, 0.300, 0.300
$x_{1U,2U}$, $y_{1U,2U}$	0.778, 0.778, 0.338, 0.338	0.778, 0.778, 0.338, 0.338
g_1, g_2	0.32	1.00
A_1, A_2	0.5	1.0
Inclination (°)	80.85±0.07	79.46±0.06
T_1, T_2 (K)	7300, 7225±2	7300, 7138±3
$\Omega_1 = \Omega_2$	2.692±0.002	2.737±0.002
$q(m_2 / m_1)$	0. 4803±0.0007	0. 478±0.001
Fill-outs: $F_1 = F_2$	50.5±0.3%	33±1%
$L_1 / (L_1+L_2)_I$	0.6569±0.0019	0.6699±0.0011
$L_1 / (L_1+L_2)_R$	0.6587±0.0014	0.6734±0.0008
$L_1 / (L_1+L_2)_V$	0.6604±0.0011	0.6773±0.0006
$L_1 / (L_1+L_2)_B$	0.6628±0.0017	0.682±0.001
$L_1 / (L_1+L_2)_U$	0. 6620±0.0019	0. 680±0.001
JD_o (days)	56199.9620±0.0002	56199.9620±0.0002
Period (days)	0.46862±0.00008	0.46862±0.00008
r_1, r_2 (pole)	0.444±0.003, 0.324±0.005	0.435±0.003, 0.314±0.005
r_1, r_2 (side)	0.479±0.004, 0.343±0.006	0.467±0.005, 0.330±0.006
r_1, r_2 (back)	0.520±0.007, 0.401±0.014	0.520±0.007, 0.377±0.012
Spot 1 On STAR 1	Cool Spot	Cool Spot
Colatitude (°)	81.9±1.4	82±4
Longitude (°)	97.4±0.9	97±6
Spot radius (°)	9.9±0.5	10±1
Spot T-factor	0.883±0.004	0.883±0.004
Spot 2 On STAR 1	Hot Spot	Hot Spot
Colatitude (°)	21.1±0.7	17±1
Longitude (°)	358.3±0.9	355±2
Spot radius (°)	23.0±0.3	23.0±0.4
Spot T-factor	1.10±0.01	1.074±0.004
Σres^2	0.42515	0.57855

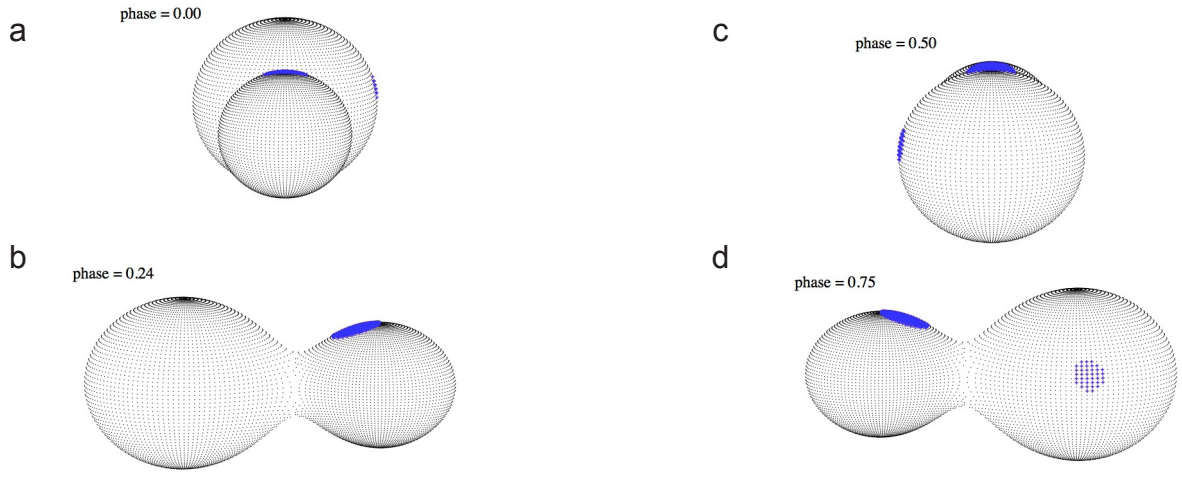

Figures 7a, 7b, 7c, 7d. Roche Lobe surfaces of V444 And.

References

Berry, R., and Burnell, J. 2011, "Astronomical Image Processing for Windows," version 2.4.0, provided with *The Handbook of Astronomical Image Processing*, Willmann-Bell, Richmond, VA.

Bradstreet, D. H., and Steelman, D. P. 2002, *Bull. Amer. Astron. Soc.*, **34**, 1224.

Diethelm, R. 2007, *Inf. Bull. Var. Stars*, No. 5781, 1.

Henden, A. A., *et al.* 2013, AAVSO Photometric All-Sky Survey, data release 7 (http://www.aavso.org/apass).

Jiang, D., Han, Z., and Li, L. 2014, *Mon. Not. Roy. Astron. Soc.*, **438**, 859.

Kazarovets, E. V., Samus, N. N., Durlevich, O. V., Kireeva, N. N., and Pastukhova, E. N. 2006, *Inf. Bull. Var. Stars*, No. 5721, 1.

Lewandowski, M., Niedzielski, A., and Maciejewski, G. 2007, *Inf. Bull. Var. Stars*, No. 5784, 1.

Nagai, K. 2004, *Var. Star Bull.* (Japan), No. 42, 1.

Nakajima, K., Yoshida, S., Ohkura, N., and Kadota, K. 2005, *Inf. Bull. Var. Stars*, No. 5600, Report No. 7.

Pejcha, O. 2005, *Inf. Bull. Var. Stars*, No. 5645, 1.

Van Hamme, W., and Wilson, R. E. 1998, *Bull. Amer. Asron. Soc.*, **30**, 1402.

Wilson, R. E. 1990, *Astrophys. J.*, **356**, 613.

Wilson, R. E. 1994, *Publ. Astron. Soc. Pacific*, **106**, 921.

Wilson, R. E., and Devinney, E. J. 1971, *Astrophys. J.*, **166**, 605.

Yakut, K., and Eggleton, P. P. 2005, *Astrophys. J.*, **629**, 1055.

Yildiz, M. 2014, *Mon. Not. Roy. Astron. Soc.*, **437**,185.